NATIONAL ADVISORY COMMITTEE FOR AERONAUTICS

TECHNICAL NOTE 2500

A COMPARISON OF THE TURBULENT BOUNDARY-LAYER GROWTH ON AN UNSWEPT AND A SWEPT WING

By John M. Altman and Nora-Lee F. Hayter

Ames Aeronautical Laboratory
Moffett Field, Calif.

Washington
September 1951

NATIONAL ADVISORY COMMITTEE FOR AERONAUTICS

TECHNICAL NOTE 2500

A COMPARISON OF THE TURBULENT BOUNDARY-LAYER GROWTH ON AN UNSWEPT AND A SWEPT WING

By John M. Altman and Nora-Lee F. Hayter

SUMMARY

In order to check the applicability of simple sweep theory to the turbulent boundary-layer growth on swept wings, an experimental investigation was undertaken in which measurements were made of the turbulent boundary layer of a two-dimensional unswept wing and a comparable wing swept 45°. The tests were conducted at a Reynolds number of about 4 million based on the component of velocity normal to the leading edge.

The experimental results indicate the applicability of simple sweep theory for determining turbulent boundary-layer growth on the swept wing for a lift coefficient of zero. For the wings at moderate lift coefficients, the growth of the boundary-layer component normal to the leading edge was more rapid on the swept wing than on the unswept wing. This difference, however, is believed to be primarily the result of differences in the surface conditions of the two models. Support is given to this belief by the fact that the growth of the momentum thickness on the swept wing calculated in accordance with simple sweep theory by using the component of flow normal to the leading edge was in good agreement with the measured growth.

INTRODUCTION

A theory has been advanced to the effect that certain aerodynamic characteristics of an infinite swept wing are determined solely by the component of velocity normal to the leading edge. (See, for example, reference 1.) Various experimental investigations have shown that this idea, commonly referred to as simple sweep theory, provides a satisfactory explanation of many of the observed characteristics of swept wings. For example, it is shown in references 2 and 3 that the chordwise distributions of pressure, and hence the lift coefficients, when based on the component of velocity normal to the leading edge, were the same for a straight wing and a swept wing. In reference 3, comparison is made of two constant-chord wings, both of which completely spanned the wind

tunnel. It was found that simple sweep theory, insofar as pressure distribution was concerned, applied to the central 40 percent of the span of the swept wing.

The purpose of the present investigation was to ascertain the applicability of simple sweep theory to turbulent boundary-layer growth. The investigation was conducted in one of the Ames 7- by 10-foot wind tunnels and employed the two models described in reference 3. The results of measurements of the turbulent boundary layer on these models are presented in this report.

NOTATION

The notation and sign conventions used in the discussion of the characteristics of the swept wing are shown in figure 1. The notation used throughout this report is defined as follows:

c	chord of wing normal to leading edge, feet
c_{l_u}	uncorrected section lift coefficient based on integrated pressure-distribution diagrams and the component of velocity normal to the leading edge
H	boundary-layer shape parameter $\left(\frac{\delta^*}{\theta}\right)$
K	$\frac{U_o \sin \Lambda}{U}\left(\frac{\theta_{yx}}{\theta_x}\right)$
P	pressure coefficient $\left(\frac{p - p_o}{q_o}\right)$
Δp_R	difference of pressures measured by outer tubes of directional rake
p	local static pressure, pounds per square foot
p_o	free-stream static pressure, pounds per square foot
q_o	free-stream dynamic pressure, pounds per square foot
q_R	dynamic pressure measured by directional rake, pounds per square foot
U	component of local velocity outside boundary layer normal to leading edge, feet per second
U_o	free-stream velocity, feet per second
u	component of local velocity inside boundary layer normal to leading edge, feet per second

V component of local velocity outside boundary layer parallel to leading edge, feet per second

v component of local velocity inside boundary layer parallel to leading edge, feet per second

x normal distance from leading edge, feet

y distance from upstream end of swept wing parallel to leading edge, feet

z distance from wing surface normal to surface, feet

δ boundary-layer thickness, feet

δ^* boundary-layer displacement thickness

$$\left[\int_0^{\delta}\left(1-\frac{u}{U}\right)dz\right] \text{ or } \left[\int_0^{\delta}\left(1-\frac{v}{V}\right)dz\right], \text{ feet}$$

θ boundary-layer momentum thickness

$$\left[\int_0^{\delta}\frac{u}{U}\left(1-\frac{u}{U}\right)dz\right] \text{ or } \left[\int_0^{\delta}\frac{v}{V}\left(1-\frac{v}{V}\right)dz\right], \text{ feet}$$

θ_{yx} $\displaystyle\int_0^{\delta}\frac{u}{V}\left(1-\frac{v}{V}\right)dz$

Λ angle of sweep, degrees

ψ angle of flow within boundary layer relative to free-stream direction, degrees

Subscripts

x based on the component of velocity normal to the leading edge

y based on the component of velocity parallel to the leading edge

MODELS AND APPARATUS

Both wings used in this investigation had NACA 63_1-012 sections perpendicular to their leading edges. The unswept wing, having a chord of 4 feet, was mounted vertically and spanned the 7-foot dimension of the wind tunnel (fig.2). The 45° swept wing, having a chord of 2.5 feet perpendicular to the leading edge, was mounted horizontally and spanned the 10-foot dimension of the wind tunnel (fig.3).

The distribution of pressure over the swept wing was measured by means of streamwise rows of pressure orifices in the surface of the model. In addition, the spanwise distribution of pressure was measured along constant-chord lines at 5, 15, 30, 50, and 80 percent of the chord. The chordwise distribution of pressure over the unswept wing was measured by a row of orifices at midspan.

The directional rake used to measure boundary-layer velocity profiles and angles of flow on the swept wing is shown in figure 4. This rake was similar to the one described in reference 4. It consisted of one static-pressure tube and three total-pressure tubes made from 0.022-inch-outside-diameter steel tubing. The total-pressure tubes were flattened to an oval shape and the open ends of the two outer tubes were cut back 30°. (See fig. 4(a).) The stem of the directional rake was sealed tightly in holes drilled through the model as shown in figure 4(b) and was clamped to the underside of the model. The rake was moved to measure the local velocity at several heights within the boundary layer at selected locations.

Calibration of the directional rake showed that the dynamic pressure, based on the readings of the center tube and the static tube of the rake, was essentially constant with yaw angles between ±20°. The slope of the angle calibration curve $[d(\Delta p_R/q_R)]/d\psi$ based on the readings of the two outer tubes was constant within the same limits.

Boundary-layer velocity profiles for the unswept wing were measured by means of small rakes, each composed of a static-pressure tube and several total-pressure tubes. The rakes were made of 0.010-inch- and 0.30-inch-outside-diameter steel tubing, the smaller tubing being used to measure boundary layers less than 0.10 inch thick.

TESTS

In order to simulate flow over an infinite yawed wing unaffected by the influence of tunnel walls, the swept wing was twisted. This twist produced a region for the measurement of turbulent boundary layers in which there was relatively no variation of pressures in the direction parallel with the leading edge (referred to in this report as the spanwise direction). The amount of twist across the span varied from no

twist for zero lift coefficient to 1.5° for a lift coefficient of 1.00. Velocity profiles within the boundary layer were measured along the mid-span section at 30, 40, 50, 60, 70, 80, and 90 percent of the streamwise chord on both wings. In addition, the flow direction within the boundary layer was determined for the swept wing. These measurements were made for section lift coefficients of 0, 0.32, 0.46, 0.74, and 1.00 based on the component of velocity normal to the leading edge. Also measured at the same lift coefficients were boundary-layer velocity profiles at various stations along the span of the swept wing at 30 percent of the chord.

In order to determine the effect of a moderate spanwise pressure gradient on the growth of the boundary layer of the swept wing, a spanwise variation of pressure was obtained by twisting the wing in a direction opposite that which eliminated the spanwise variation. The amount of twist was limited to 1.5° by the strength of the model. Additional measurements of the velocity profiles at several spanwise stations were then made at 30 percent of the chord.

For zero lift the transition point from laminar to turbulent flow did not occur at the same chordwise station for the swept wing as for the unswept wing, nor did it occur uniformly along the span of the swept wing. To insure comparable results with the wing at zero lift, transition was artificially induced by applying roughness along the span of each wing between 18 and 20 percent of the chord. This roughness consisted of a dense coating of number 60 carborundum granules glued to a 3/4-inch-wide strip of cellulose tape. At moderate lift coefficients transition occurred naturally near the leading edges of both wings and, therefore, artificial roughness was not applied.

An attempt was made to maintain similar surface conditions for both wings; however, the swept wing had some seams near the leading edge that were difficult to keep smooth, and this roughness may have increased the thickness of the boundary layer.

Tunnel-wall corrections were not applied to the lift coefficients of either wing. The tests of the swept wing were conducted at a dynamic pressure of 150 pounds per square foot and those of the unswept wing, at a dynamic pressure of 29.5 pounds per square foot. The Reynolds number based on the component of velocity normal to the leading edge was about 4 million for both wings.

RESULTS AND DISCUSSION

Growth of the Chordwise Boundary-Layer Component

Wings at zero lift with transition fixed.- Distributions of the pressure coefficients over the upper surfaces of the wings are shown

in figure 5 for a lift coefficient of zero. The streamwise pressure coefficients for the swept wing have been divided by the $\cos^2 45^\circ$ in order to base these coefficients on the component of velocity normal to the leading edge. On this basis, the pressure distribution of the swept wing shows good agreement with that of the straight wing.

In the following section the growth of the boundary layer on the swept wing, although actually measured along a streamwise section of the wing, will be referred to as the chordwise growth of the boundary layer. It is believed that the constancy of the spanwise distribution of pressure over the central portion of the wing would insure identical boundary-layer growth along any section of the wing within this region.

A comparison between the velocity profile within the boundary layer at 50 percent of the chord for the unswept wing and those based on the components of velocity normal and parallel to the leading edge of the swept wing at the same chord station is shown in figure 6. The chordwise growth of the displacement thickness, the momentum thickness, and the shape parameters obtained from velocity-ratio profiles in the x direction similar to those presented in figure 6 are shown in figure 7 for both wings. The data presented in figures 6 and 7 were obtained with roughness strips on the surface of each wing between 18 and 20 percent of the chord. Although there were some differences in the shapes of the boundary-layer velocity profiles on the swept and the unswept wing (fig. 6), the derived boundary-layer parameters (fig. 7) show reasonably good agreement from 30 to 90 percent of the chord.

In figure 8 is shown the direction of flow within the boundary layer for various percent-chord stations of the swept wing. Near the surface the flow over the forward part of the wing tended toward the upstream end of the wing, and turned toward the downstream end over the rear portion of the wing. Throughout the outer half of the boundary layer the direction of flow tended toward the upstream end but approached the free-stream direction as the boundary-layer flow approached the trailing edge.

A comparison of the displacement thickness, the momentum thickness, and the shape parameter based on the components of velocity normal to and parallel to the leading edge of the swept wing at zero lift shows that for this condition the parameters in the two planes are similar (fig. 9). The velocity-ratio profiles, however, were different (fig. 6).

Wings at moderate lift coefficient.- In figure 10 are shown the pressure-coefficient distributions over the upper surface of the unswept wing together with those of the swept wing based on the component of velocity normal to the leading edge. The pressure distributions correspond to section lift coefficients of 0.32, 0.46, 0.74, and 1.00. The differences in the pressure coefficients near the leading edge are believed to have been due to small differences in the contours of the models. A comparison of typical velocity-ratio profiles measured at

50 percent of the chord for a section lift coefficient of 0.74 for both the swept and the unswept wings is shown in figure 11. The boundary-layer parameters for the swept and the unswept wings are shown in figure 12. The shape parameters H_x are approximately the same for both wings; however, the displacement and the momentum thicknesses for the swept wing had greater values at 30-percent chord and consequently greater rates of growth along the chord.

The major factors that might be expected to affect the values of the boundary-layer parameters at moderate lift coefficients are the spanwise pressure gradient, the surface conditions, the small differences in the chordwise pressure distributions over the upper surface of the swept and unswept wings, and the Reynolds number. An attempt was made to ascertain the effect of an increased spanwise pressure gradient on the momentum thickness at 30 percent of the chord by twisting the swept wing to obtain a more pronounced spanwise pressure gradient (fig. 13(b)). The results show no change in the momentum thickness at 30-percent chord (fig. 13(c)). These data, however, are not conclusive proof that the spanwise pressure gradient did not account for the increased values of the momentum thickness for the swept wing since twisting the wing to produce a more pronounced spanwise pressure gradient also reduced the adverse pressure gradient along the forward 30 percent of the chord at midspan. This reduction of the adverse pressure gradient would tend to reduce the thickness of the boundary layer at 30-percent chord, and therefore might have counteracted any tendency of the increased spanwise pressure gradient to increase the thickness.

The greater thickness of the boundary layer on the swept wing may also have been due to the differences in the surface conditions of the two models.

Since it was not feasible to determine the applicability of simple sweep theory to turbulent boundary layers by a direct comparison of the boundary-layer parameters measured for these swept and unswept wings at finite lift coefficients, it was necessary to use an indirect method.

According to simple sweep theory, certain aerodynamic characteristics of a swept wing are dependent solely on the component of velocity normal to the leading edge. Therefore, it was believed that if the boundary-layer parameters for the swept wing could be computed accurately considering only this component of velocity, it could be inferred that simple sweep theory was applicable to turbulent boundary-layer growth on a swept wing at moderate lift coefficients. The method of reference 5, based on the pressure distribution, the Reynolds number, and the initial momentum thickness, was found to predict the growth of momentum thickness for the swept wing with fair accuracy (see fig. 14). Having determined that this method gave reasonably good results in the case of the unswept wing, it was then used to compute the growth of momentum thickness on the swept wing in a plane normal to the leading edge using the velocity distribution, the shape parameter, the Reynolds number, and the

experimentally determined momentum thickness at 30-percent chord. A comparison of these predicted values with the experimental values for the swept wing based on the component of velocity normal to the leading edge is shown in figure 15. The agreement for the swept wing is of the same order of accuracy as for the unswept wing, thereby giving support to the belief that simple sweep theory is applicable to turbulent boundary-layer growth for moderate lift coefficients.

For the swept wing, the angles of flow within the boundary layer are shown in figure 16 for lift coefficients of 0.32, 0.46, 0.74, and 1.00. The greatest effect of increased lift coefficient on the flow direction within the boundary layer was near the surface of the model over the rear portion of the chord. At 90 percent of the chord, the angle of flow increased with increasing lift coefficient and reached 28° for a lift coefficient of 1.00. The boundary-layer parameters based on the component of velocity parallel to the leading edge deviated along the chord from those based on the component normal to the leading edge (fig. 17), this deviation increasing with increasing lift coefficient. It is interesting to note that there was no chordwise variation in the shape parameter H_y for a given lift coefficient.

Growth of the Spanwise Boundary-Layer Component

In reference 6 a method is derived for computing the profile drag (per unit span) of an infinite swept wing. The profile drag is considered as the resultant of two components: one normal to the leading edge (the chordwise component) and the other parallel with the leading edge (the spanwise component). Established two-dimensional-theory methods are employed for computing the chordwise growth of the boundary layer, and equations are derived for the spanwise boundary layer. The assumptions made, in addition to the usual assumptions involved in the development of two-dimensional boundary-layer equations are that the form of the spanwise velocity distribution in the boundary layer is independent of the chordwise pressure distribution and everywhere satisfies the 1/7-power law. The equations are integrated to obtain the two components of drag and these components are added vectorially to yield the resultant drag.

For turbulent flow, the equation for the spanwise component of drag (which is entirely due to surface shear since there can be no form drag in the spanwise direction) reduces to an expression involving one variable θ_{yx} which is defined as

$$\theta_{yx} = \int_0^{\delta} \frac{u}{V}\left(1 - \frac{v}{V}\right) dz$$

For the assumptions made regarding the spanwise flow θ_{yx} is shown to be related to θ_x by a factor K which is a function of H_x only.

$$\theta_{yx} = \frac{U}{U_o \sin \Lambda} K \theta_x$$

or

$$K = \frac{U_o \sin \Lambda}{U} \frac{\theta_{yx}}{\theta_x}$$

$$= \frac{U_o \sin \Lambda}{U} \frac{1}{\theta_x} \int_o^\delta \frac{u}{V} \left(1 - \frac{v}{V} \right) dz$$

In reference 6, it is suggested that values of K be computed using one of the one-parameter families of turbulent boundary layers such as that of reference 7. However, with the assumption of simple power-law velocity profiles, K can be computed more simply.

Since

$$\Lambda = 45^\circ, \; U_o \cos \Lambda = V \equiv U_o \sin \Lambda$$

and from the assumptions involved and the power-law boundary-layer relationships

$$\delta_x = \delta_y = \delta$$

$$\frac{v}{V} = \left(\frac{z}{\delta} \right)^{\frac{1}{7}}$$

$$\frac{u}{U} = \left(\frac{z}{\delta} \right)^{n}$$

where

$$n = \frac{H+1}{2}$$

hence

$$K = \frac{V}{U} \frac{1}{\theta_x} \frac{U}{V} \int_o^\delta \frac{u}{U} \left(1 - \frac{v}{V} \right) dz$$

$$= \frac{\delta}{\theta_x} \int_o^1 \left(\frac{z}{\delta} \right)^n \left[1 - \left(\frac{z}{\delta} \right)^{\frac{1}{7}} \right] d\left(\frac{z}{\delta} \right)$$

$$= \frac{\delta}{\theta_x} \left[\frac{1}{n+1} - \frac{1}{n+1+(1/7)} \right]$$

but

$$\frac{\delta}{\theta_x} = \frac{(n+1)(2n+1)}{n}$$

so

$$K = \frac{1/7}{n} \frac{2n+1}{1+n+(1/7)}$$

n	H_x	K
1/7	1.28	1.000
1/5	1.40	.745
1/4	1.50	.616
1/3	1.67	.484
1/2	2.00	.348

The data of the present investigation afforded an opportunity to compare experimentally determined values of K with these computed values. The boundary-layer measurements of the present investigation were converted into the parameters θ_{yx} and θ_x. The experimental values of K were computed from the relationship

$$K = \frac{U_o \sin \Lambda}{U} \frac{\theta_{yx}}{\theta_x}$$

where

$$\frac{U_o \sin \Lambda}{U}$$

was obtained from the measured values of the pressure distribution. A comparison of the experimentally determined values of K with those computed for velocity profiles varying according to the power law shows agreement for H_x greater than 1.5 (fig.18). The value K was also computed by using the method of reference 6 and, as shown in figure 18, this method gives larger values of K than those computed according to the power law. Considering the assumptions made in the development of this method of reference 6, the agreement between experiment and theory is reasonably good so that this method would be useful in predicting values of the profile drag of an infinite swept wing.

CONCLUDING REMARKS

Measurements were made of the turbulent boundary layers on an unswept wing and a comparable wing swept 45° for the purpose of determining the applicability of simple sweep theory to turbulent boundary-layer growth. For zero lift, with transition artificially fixed near the leading edges of both wings, it was found that the boundary-layer displacement thickness, momentum thickness, and shape parameters based on the component of velocity normal to the leading edge of the swept wing agreed well with the same parameters for the unswept wing. For lift coefficients greater than zero, with natural transition, the boundary-layer growth on the swept wing was more rapid than on the unswept wing. It was believed that this difference was due to dissimilar surface conditions for the two models. It was possible to use the two-dimensional momentum equation to calculate the growth of the turbulent boundary layer on the swept wing, with as good accuracy as on the unswept wing, by using the experimentally determined values of momentum thickness at 30 percent of the chord and by considering only the component of flow normal to the leading edge. It is indicated, therefore, that simple sweep theory is applicable to the growth of the turbulent boundary layer on a swept wing for moderate values of the lift coefficient.

A method for computing the profile drag of an infinite swept wing derived by Young and Booth involved the determination of a parameter θ_{yx} which is related to θ_x by a factor K. The data of the present investigation afforded an opportunity to compare experimentally determined values of K with those computed by the method of Young and Booth. The agreement was reasonably good and hence this method should be useful in predicting the profile drag of an infinite swept wing.

Ames Aeronautical Laboratory
National Advisory Committee for Aeronautics
Moffett Field, Calif., July 30, 1951.

REFERENCES

1. Jones, R. T.: Effects of Sweep-Back on Boundary Layer and Separation. NACA Rep. 884, 1947. (Formerly TN 1402)

2. Gothert, B.: High-Speed Measurements on a Swept-Back Wing (Sweepback Angle φ = 35). NACA TM 1102, 1947

3. Dannenberg, Robert E.: Measurements of Section Characteristics of a 45° Swept Wing Spanning a Rectangular Low-Speed Wind Tunnel as Affected by the Tunnel Walls. NACA TN 2160, 1950.

4. Weske, John R.: Experimental Investigation of Velocity Distributions Downstream of Single Duct Bends. NACA TN 1471, 1948.

5. Tetervin, Neal: A Method for the Rapid Estimation of Turbulent Boundary-Layer Thicknesses for Calculating Profile Drag. NACA ACR L4G14, 1944.

6. Young, A. D., and Booth, T. B.: The Profile Drag of Yawed Wings of Infinite Span. Coll. Aero, Cranfield, Rep. No. 38.

7. von Doenhoff, Albert E., and Tetervin, Neal: Determination of General Relations for the Behavior of Turbulent Boundary Layers. NACA Rep. 772, 1943.

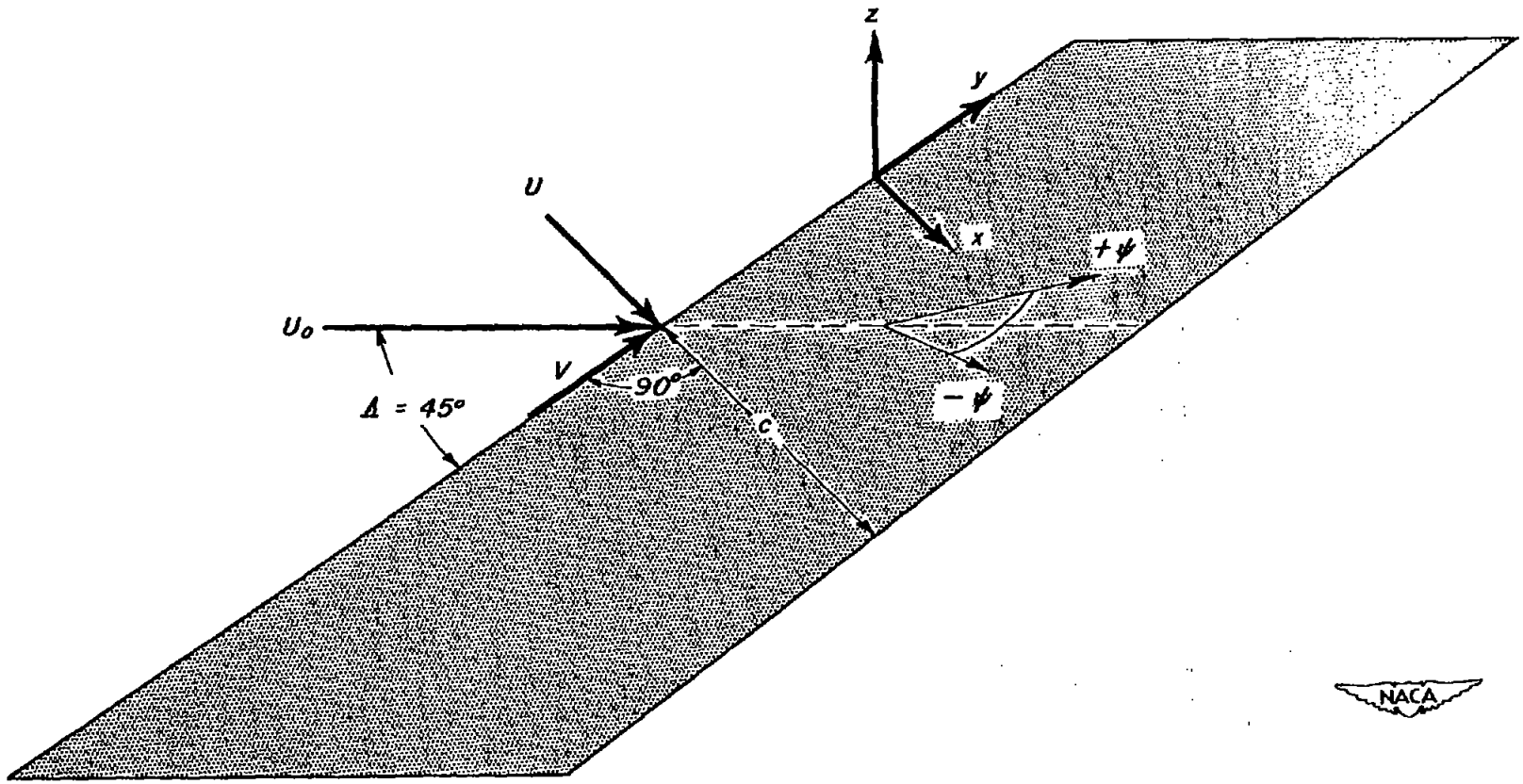

Figure 1.- Notation and sign conventions used in discussion of swept-wing characteristics.

Figure 2.– The two-dimensional unswept wing installed in the wind tunnel.

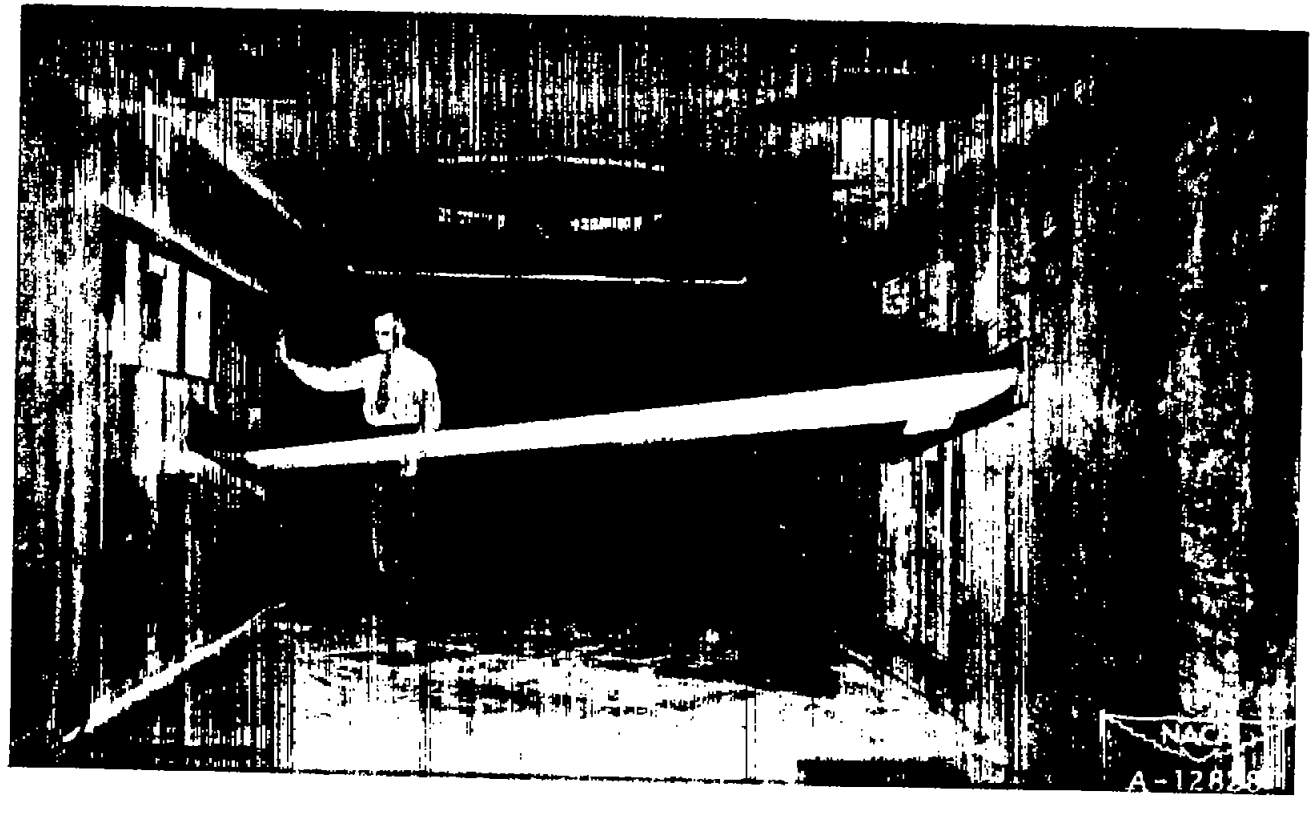

Figure 3.- The swept wing installed in the wind tunnel.

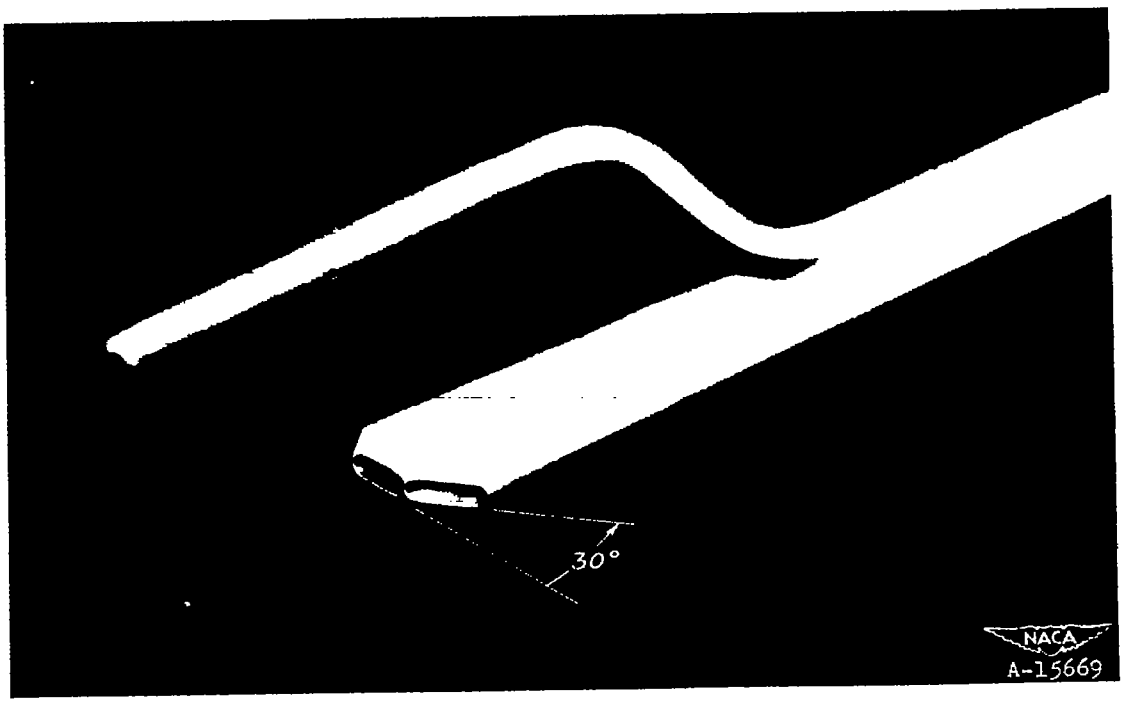

(a) Isometric sketch of rake.

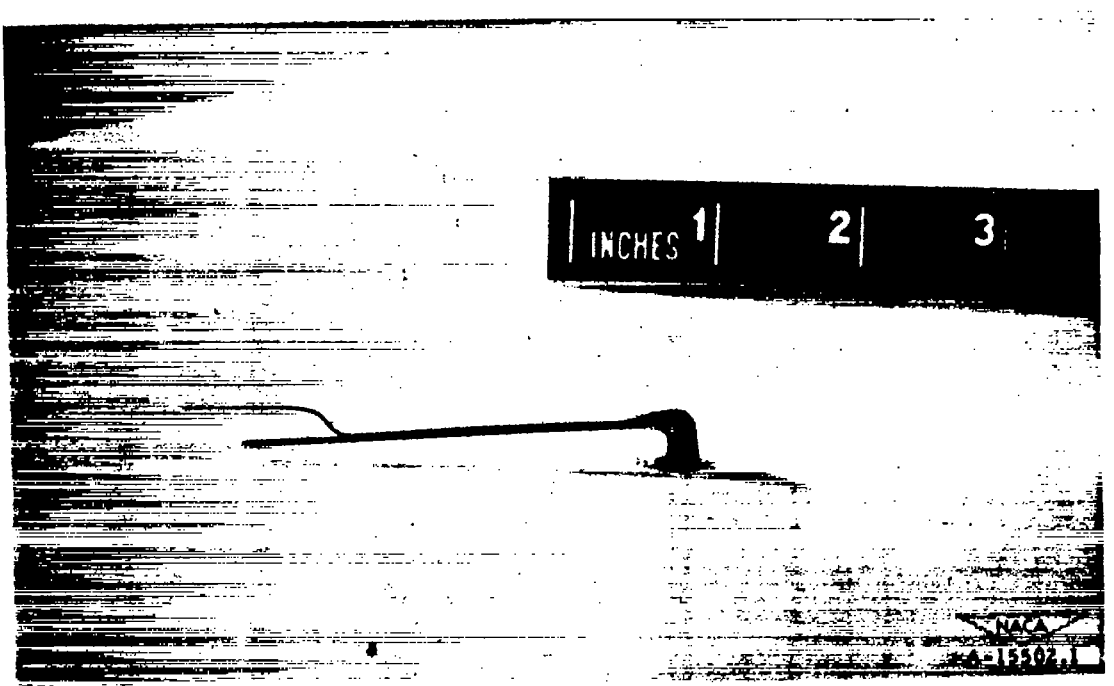

(b) Rake mounted on model.

Figure 4.- The directional rake used to measure boundary layers on the swept wing.

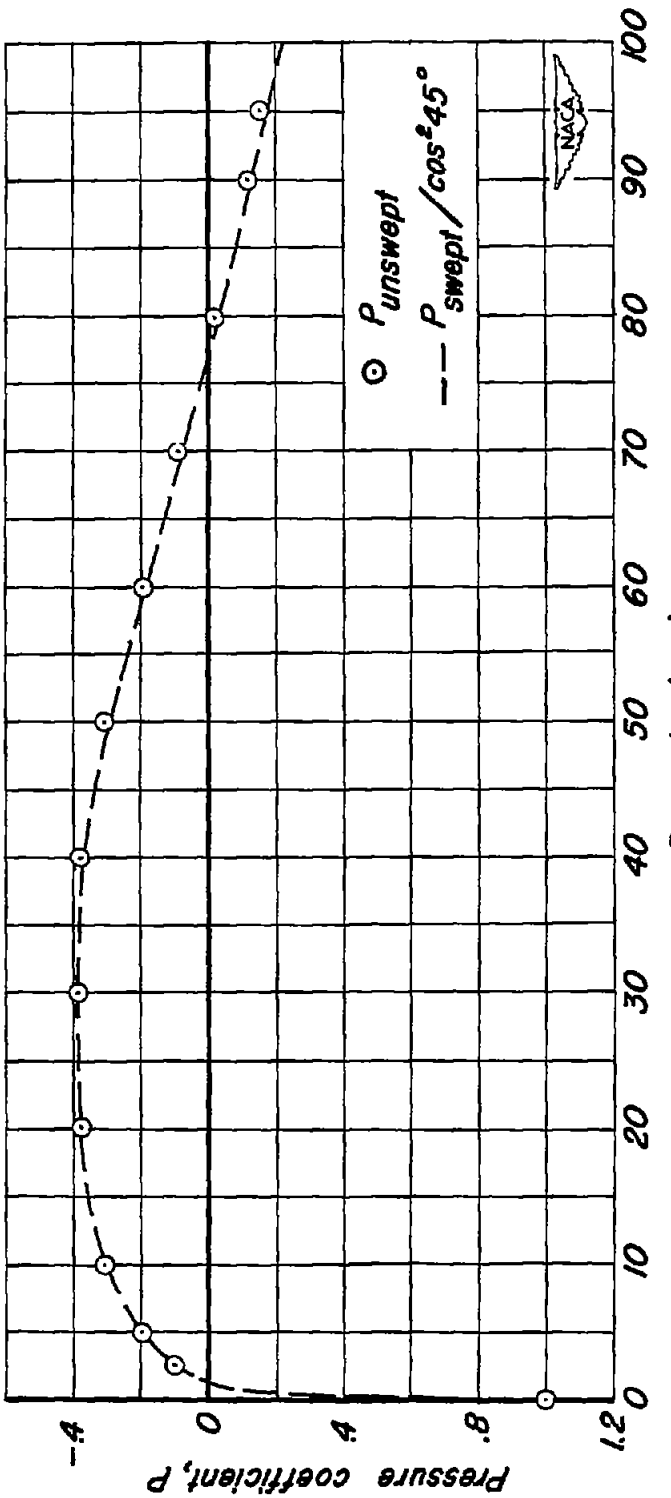

Figure 5.- Chordwise distributions of pressure over the upper surfaces of the wings. $c_{l_u} = 0$.

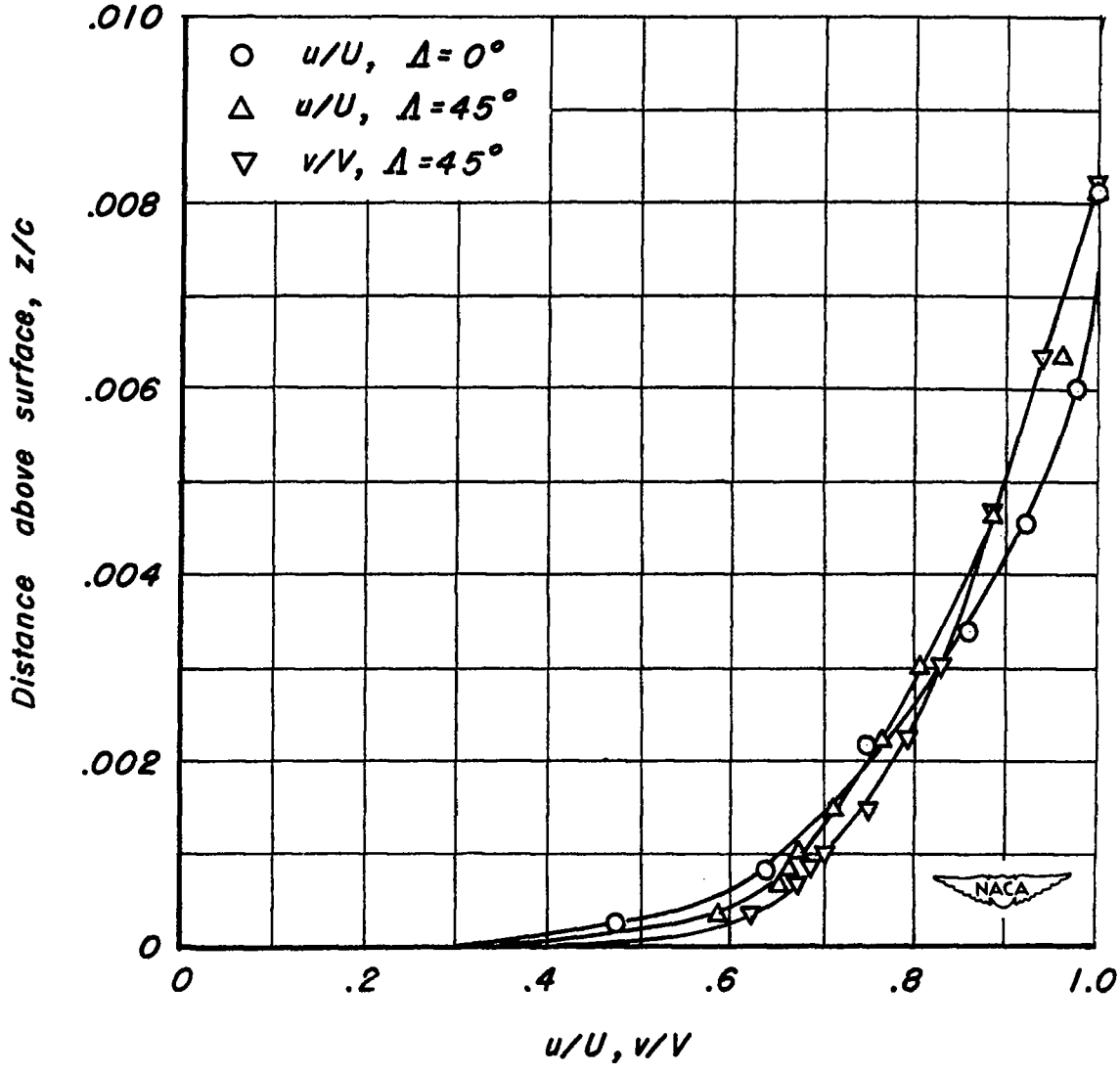

Figure 6.— Typical boundary-layer velocity profiles for the swept and the unswept wing. $c_{l_u} = 0$, $x/c = 0.50$.

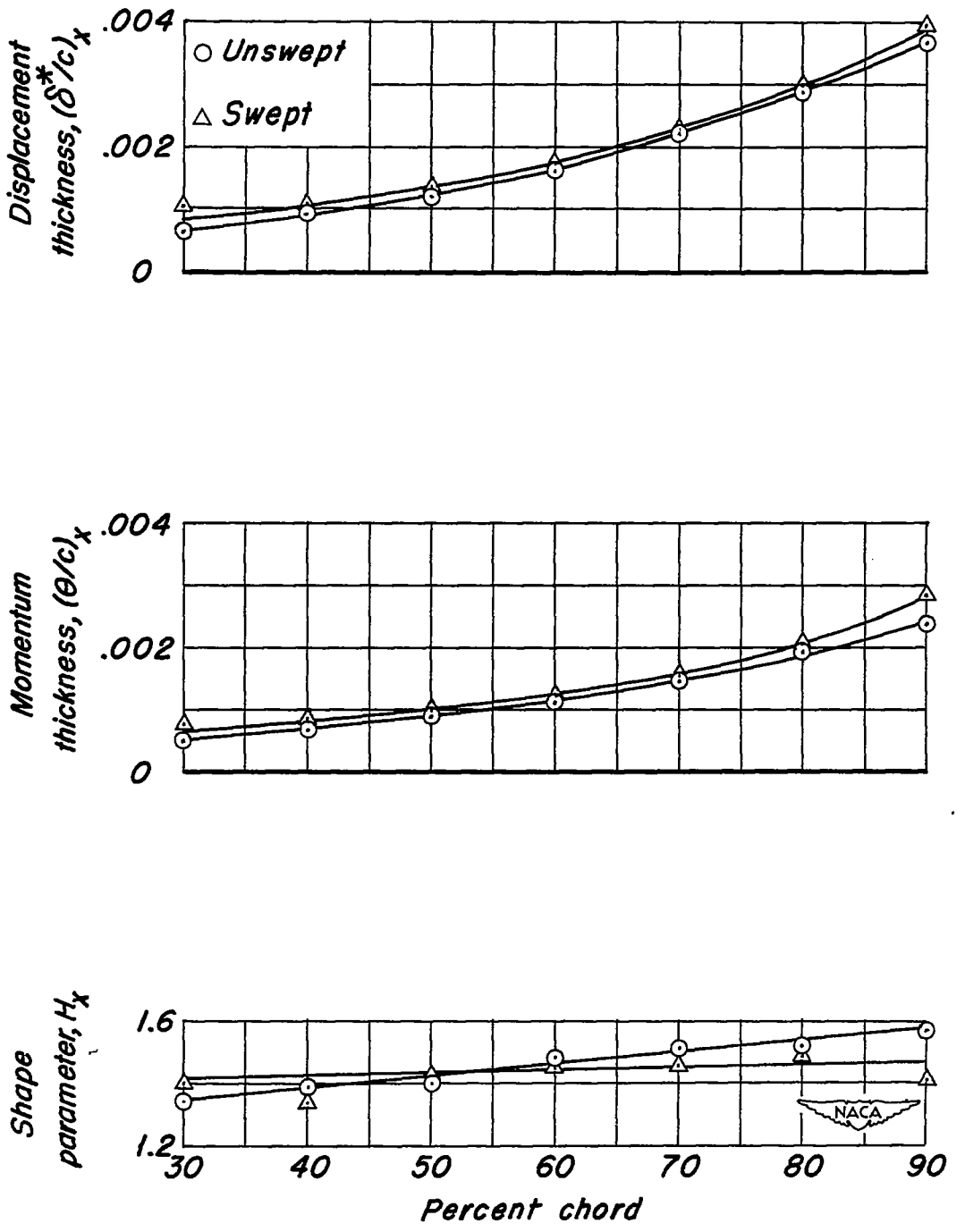

Figure 7.— Chordwise variation of three boundary-layer parameters for the swept and the unswept wing. $c_{l_u} = 0$.

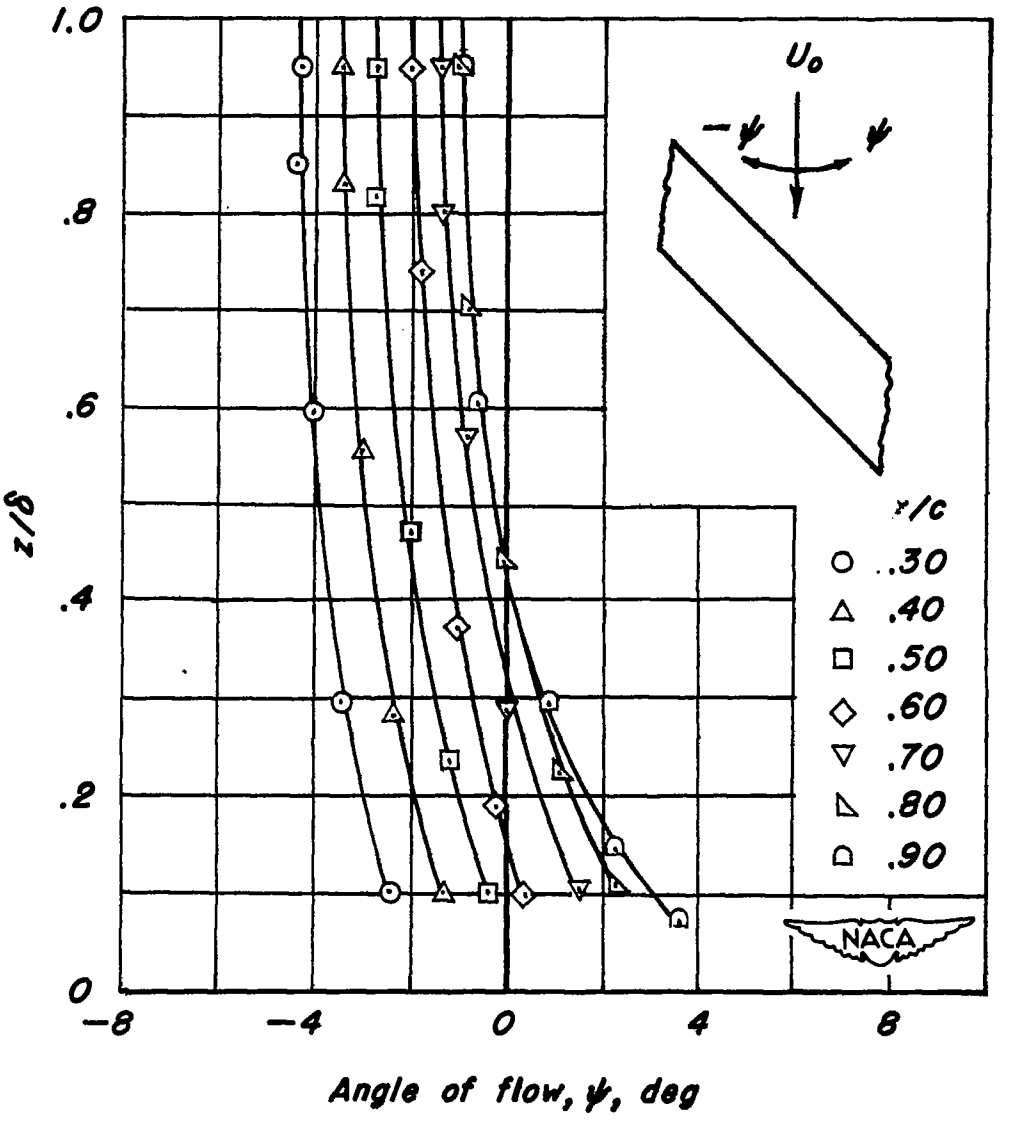

Figure 8.- Variation of angle of flow within the boundary layer of the swept wing. $c_{l_u} = 0$.

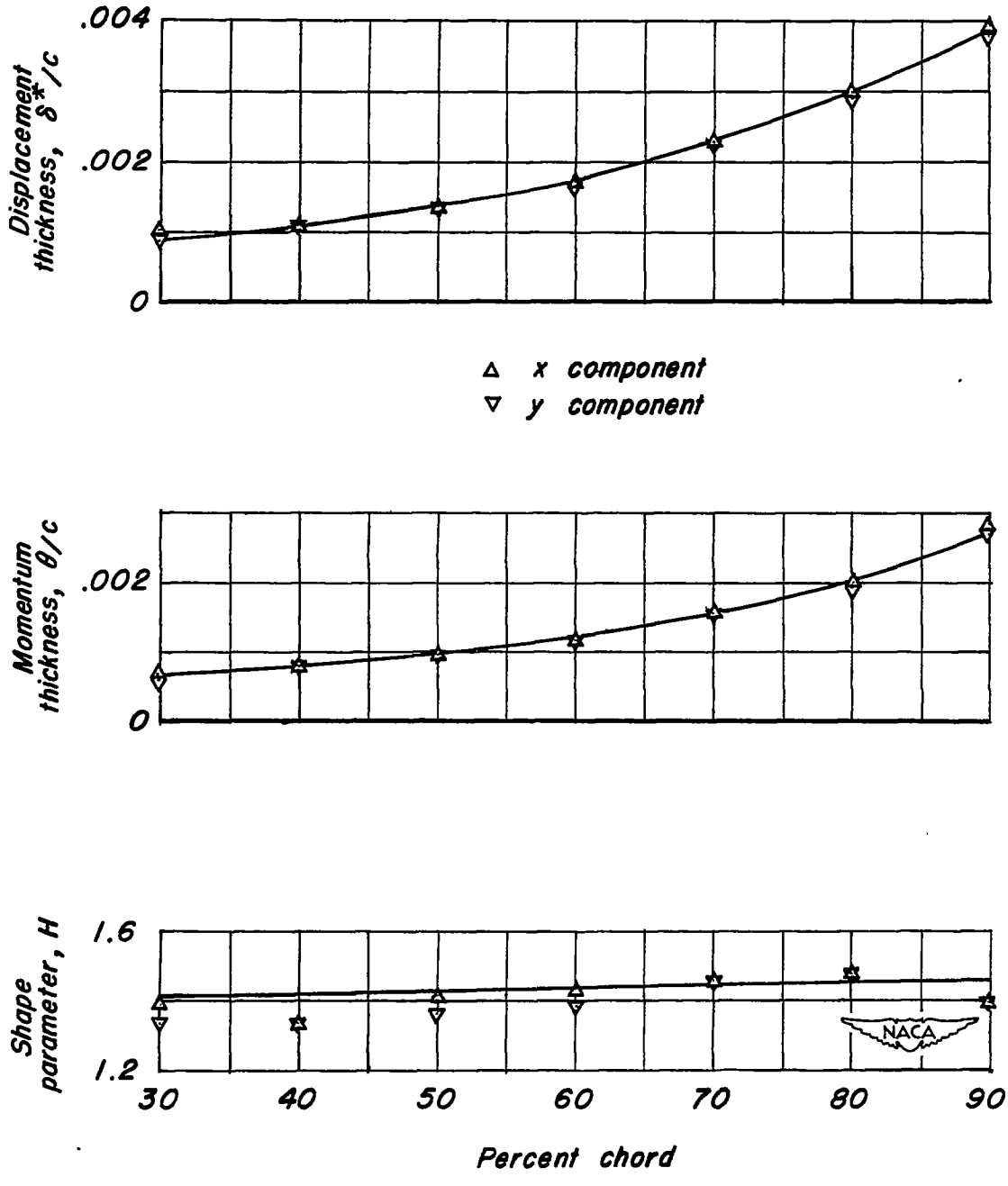

Figure 9.- Comparison of the boundary-layer parameters for the swept wing based on the x- and the y components of velocity. $c_{l_u} = 0$.

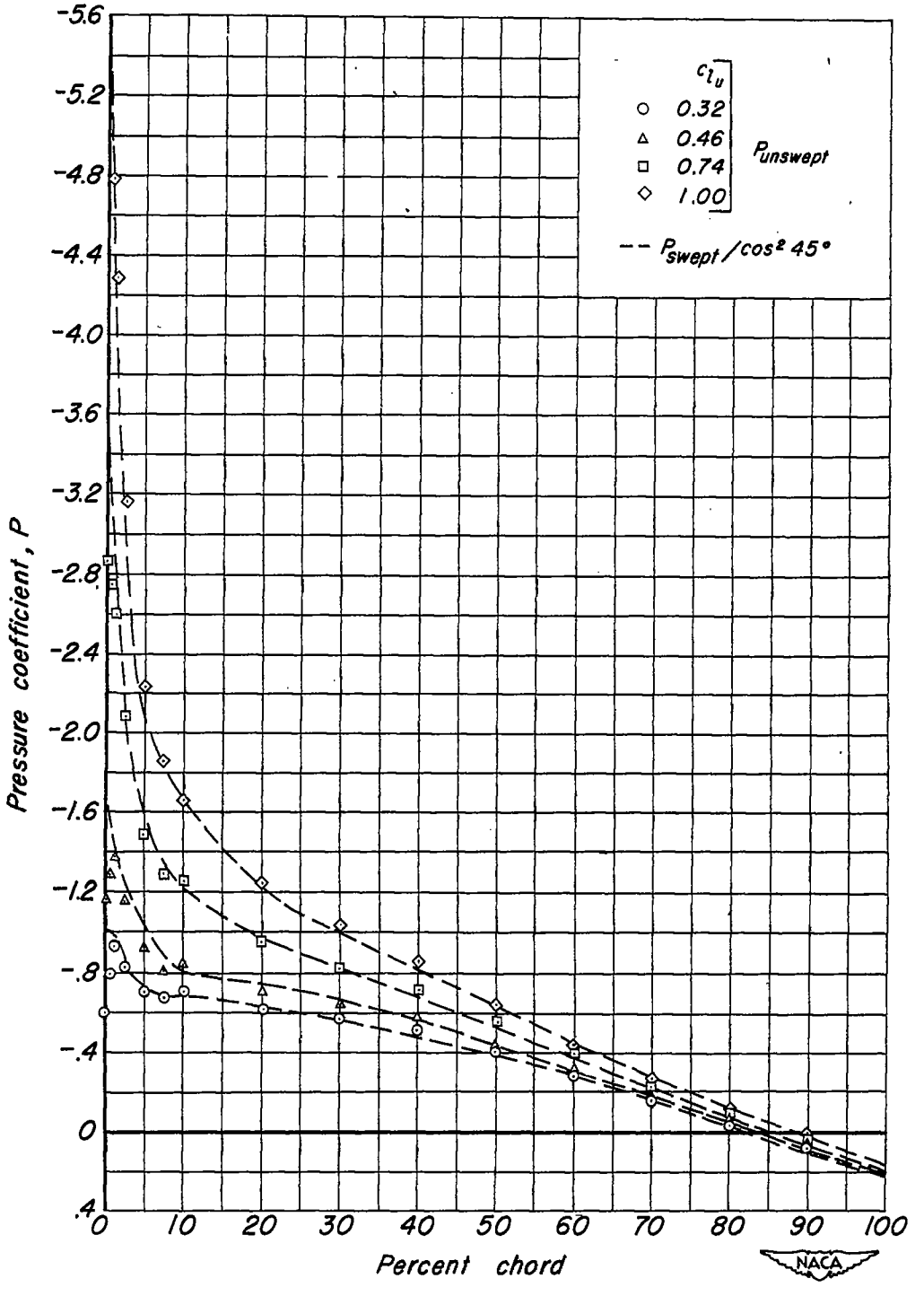

Figure 10.- Chordwise distributions of pressure over the upper surfaces of the swept and the unswept wing.

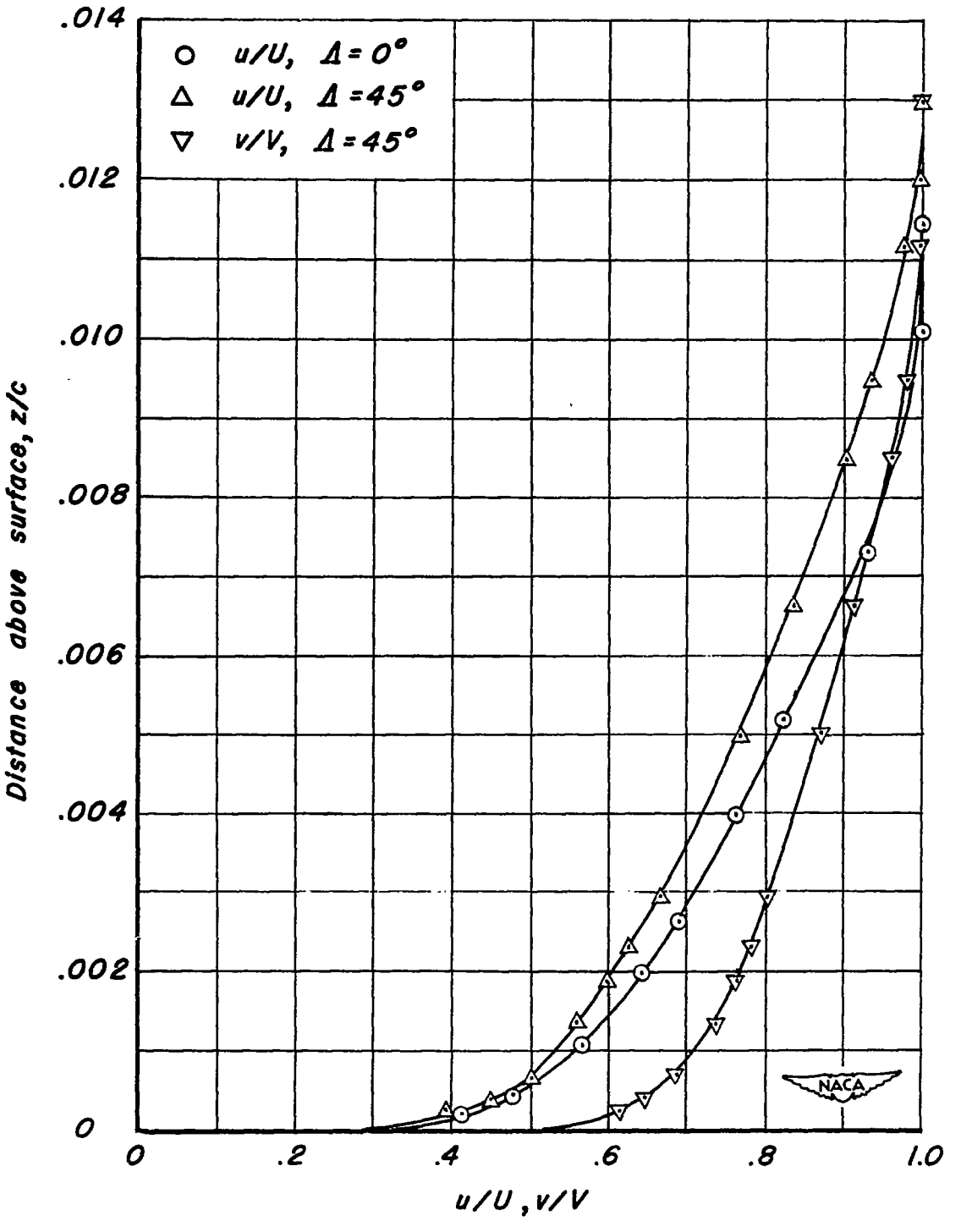

Figure 11.– Typical boundary-layer velocity profiles for the swept and the unswept wing. c_{l_u} = 0.74, x/c = 0.50.

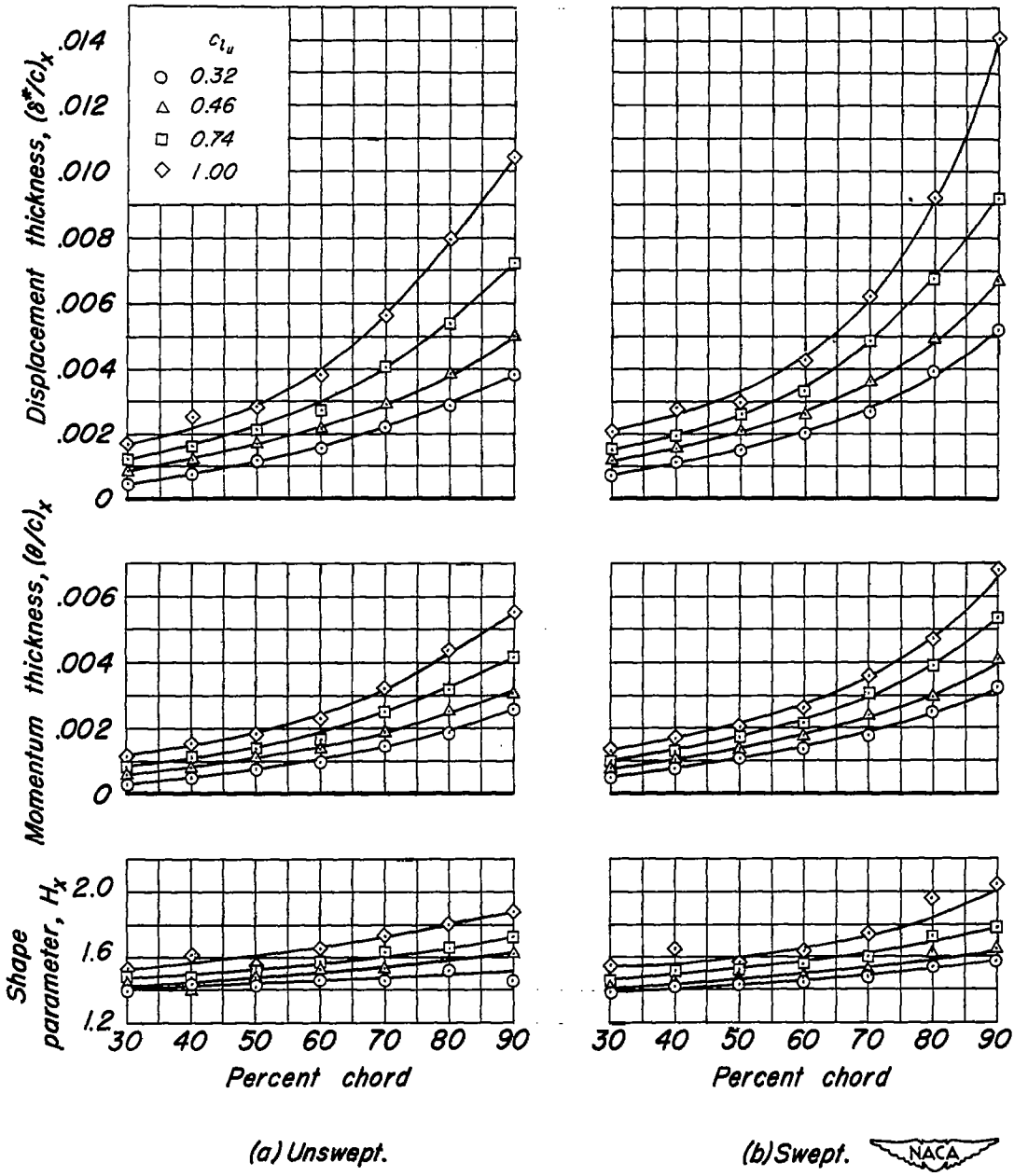

Figure 12.- Chordwise variation of three boundary-layer parameters for the swept and the unswept wing for four lift coefficients.

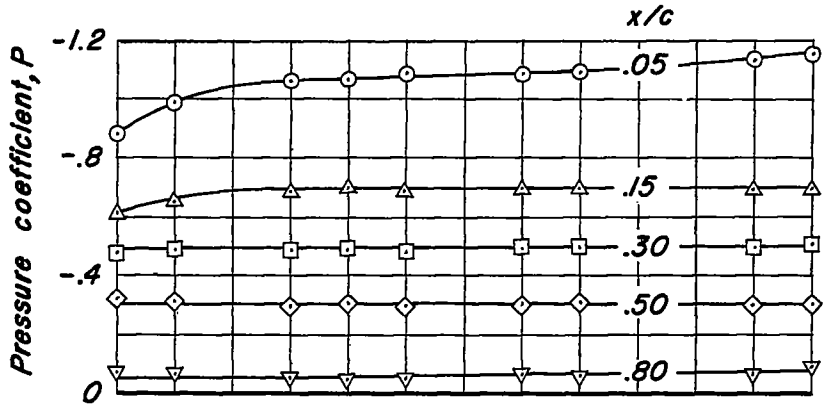

(a) Wing twisted for minimum spanwise pressure gradient

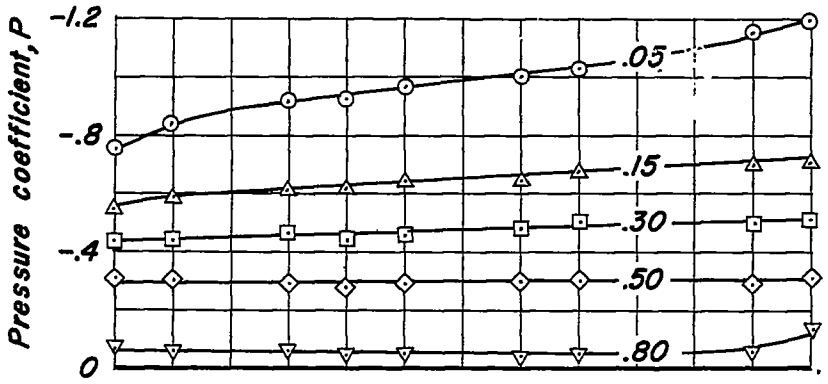

(b) Wing twisted for spanwise pressure gradient

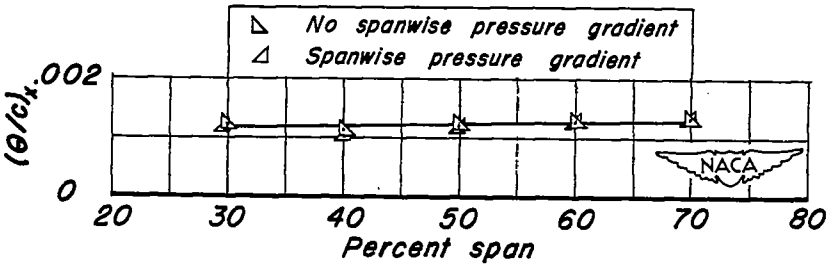

(c) Momentum thickness corresponding to conditions for (a) and (b). x/c = 0.30.

Figure 13.– Spanwise variation of the pressure coefficient and the momentum thickness for the swept wing. c_{l_u} = 1.00.

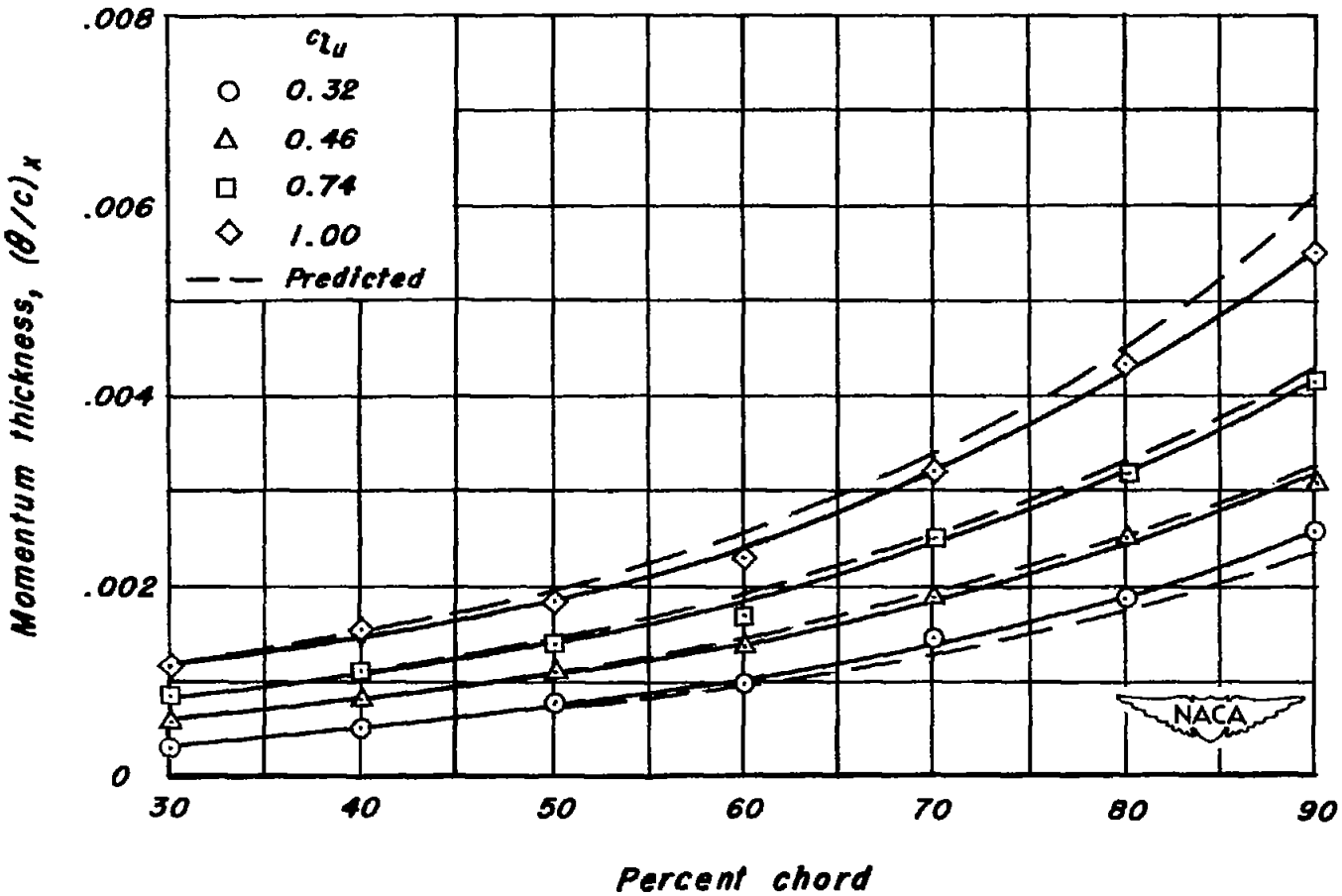

Figure 14.— Comparison of the experimental and the predicted growth of the momentum thickness for the unswept wing.

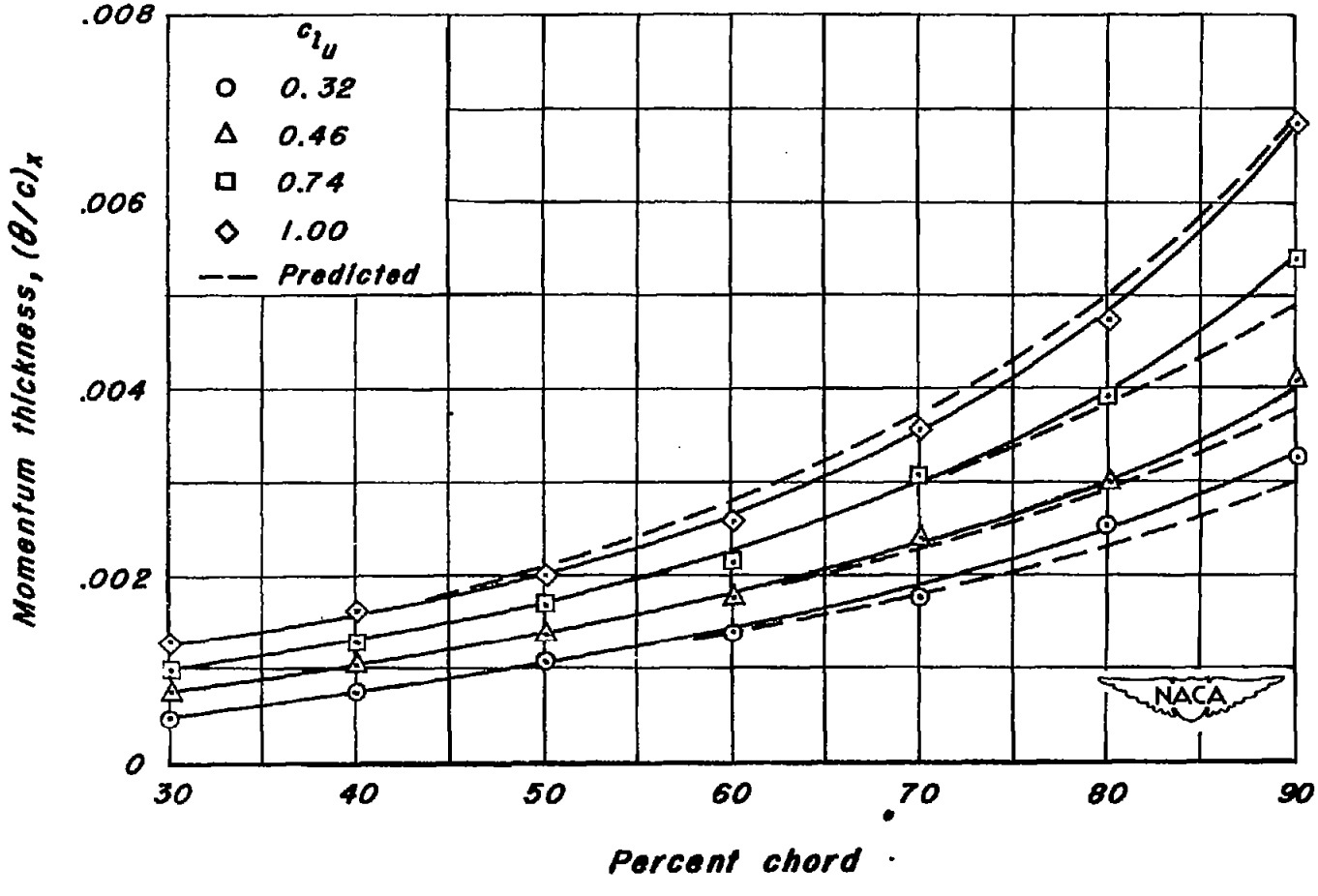

Figure 15.– Comparison of the experimental and the predicted growth of the momentum thickness for the swept wing.

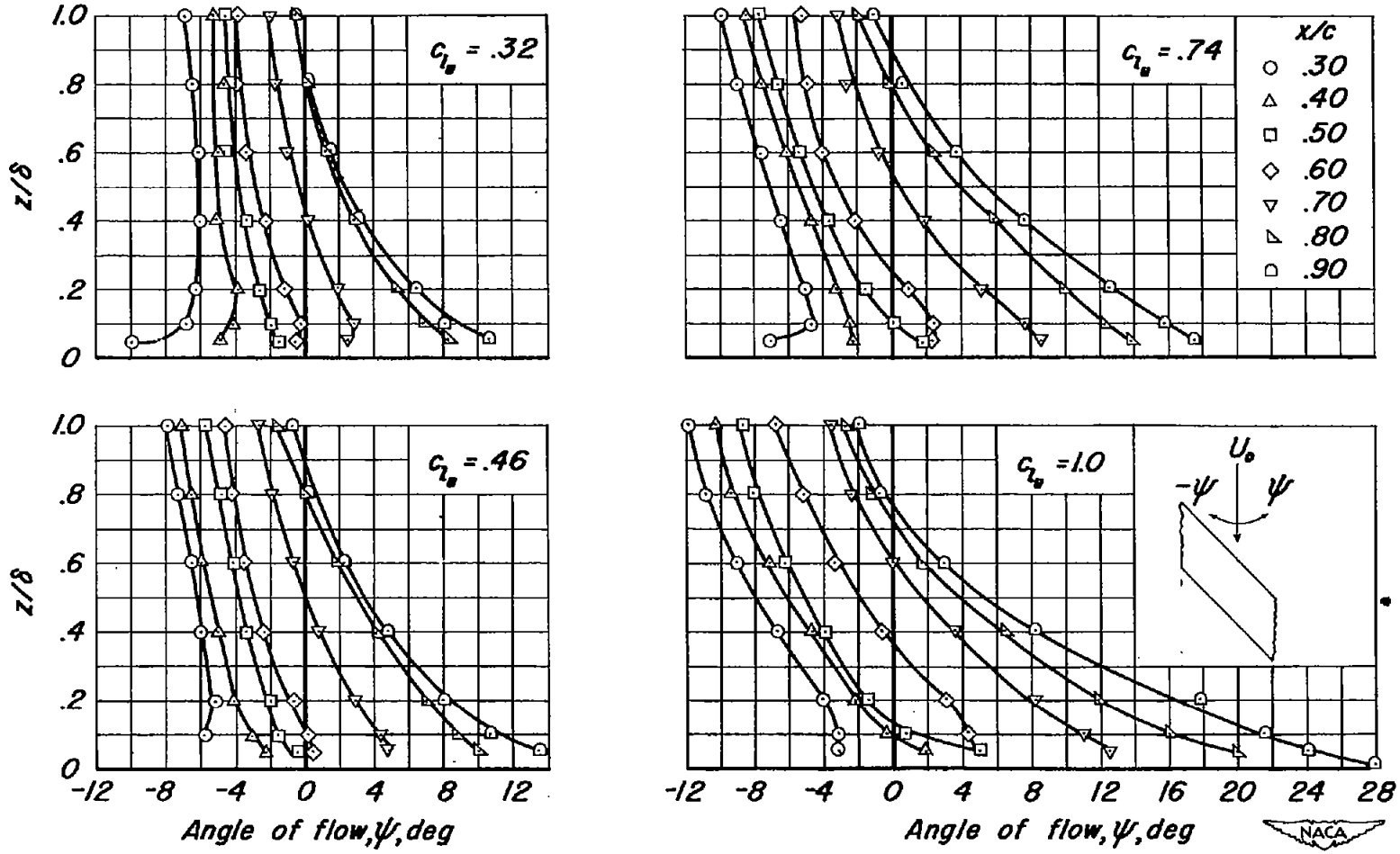

Figure 16.– Variation of angle of flow within the boundary layer of the swept wing.

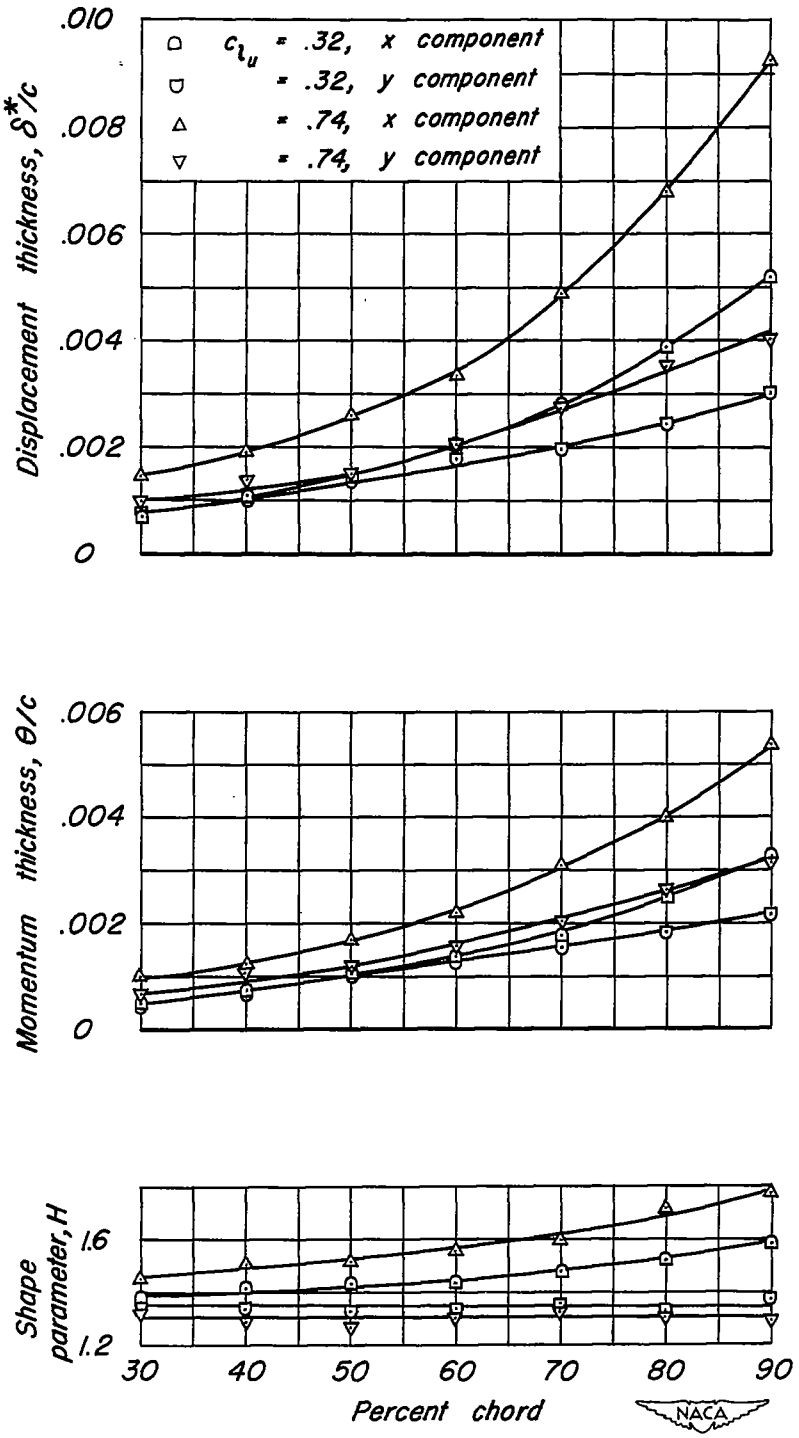

Figure 17.— Comparison of the boundary-layer characteristics of the swept wing based on the x and the y components of velocity.

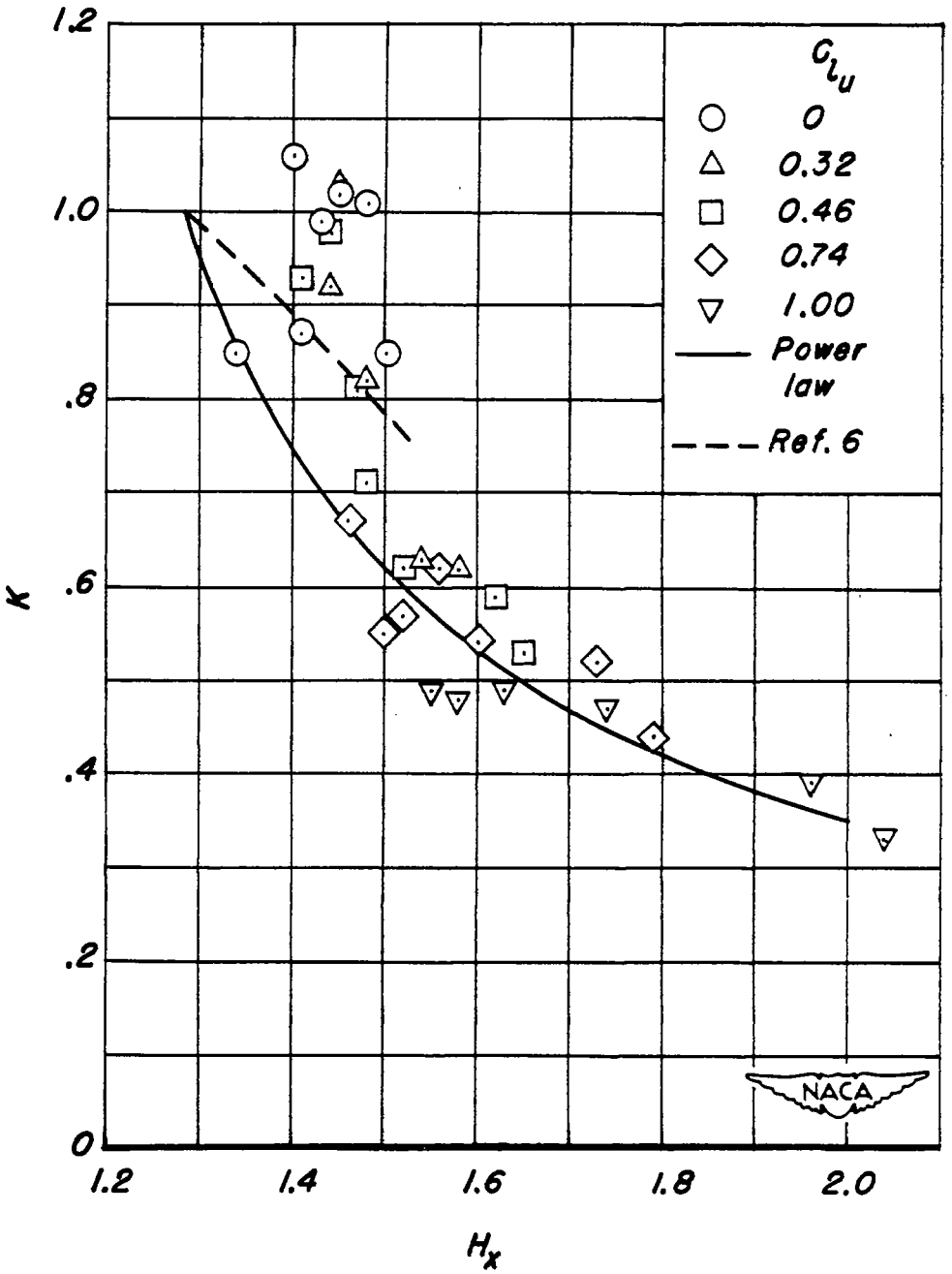

Figure 18.— Comparison of calculated and experimental values of K for the swept wing.